Astron. Astrophys. 244, 425–432 (1991)

ASTRONOMY AND ASTROPHYSICS

Abundances of neutron capture elements in metal-poor dwarfs

I. Yttrium and zirconium*

G. Zhao[1,2] and P. Magain[3,]**

[1] European Southern Observatory, Karl-Schwarzschild-Strasse 2, D (West)-8046 Garching bei München, Federal Republic of Germany

[2] Department of Astronomy, Nanjing University, Nanjing, People's Republic of China

[3] Institut d'Astrophysique, Université de Liège, 5, avenue de Cointe, B-4000 Liège, Belgium

Received August 6, accepted October 17, 1990

Abstract. The yttrium and zirconium abundances are determined in a sample of 20 metal-poor stars on the basis of high resolution, high signal-to-noise spectra. Significant differences between the behaviours of these two neighbouring elements are found, zirconium being less deficient than yttrium in Population II stars. Moreover, there is a genuine cosmic scatter in the abundances of these two elements relative to iron, of the order of 20%. The scatter is lower when these elements are compared to titanium, which might indicate that a significant fraction of the lighter neutron-capture elements are produced in massive stars.

Key words: stellar abundances – population II stars – elements: Y, Zr – nucleosynthesis – chemical evolution of the Galaxy

1. Introduction

The determination of the abundances of the chemical elements in the atmospheres of stars of different ages allows to investigate the chemical evolution of the Galaxy. The classical method consists in plotting some relative abundance against some metallicity index for a large number of stars of various overall metallicities – and thus various ages. The predictions of several chemical evolution models are then compared to the mean trend observed which, hopefully, allows to discriminate between the different models.

The combination of efficient detectors, such as the CCD, with high resolution spectrographs now allows high quality data to be obtained for stars covering a wide range in overall metallicity. Moreover, the availability of an increasing number of precise oscillator strengths for several key elements means not only that accurate trends can be obtained and compared to the models, but also that one can hope to determine the cosmic scatter in these relative abundances, thus adding a new dimension to our picture of the galactic chemical evolution.

Send offprint requests to: P. Magain

* Based on observations collected at the European Southern Observatory (La Silla, Chile)

** Chercheur Qualifié au Fonds National Belge de la Recherche Scientifique

According to the standard nucleosynthesis models, the elements heavier than the iron peak are produced by neutron capture in two main regimes (rapid or slow, the so-called r or s-processes) according to the strength of the neutron flux. To first order, the r-process isotopes are considered primary nucleosynthesis products, which means that they can be synthesized in a star of zero initial metallicity. On the other hand, the s-process isotopes are secondary products and can thus be synthesized only in a star already containing some quantity of 'seed' (iron-peak) nuclei. Since most s-process elements – especially the heavier ones – are thought to be produced mainly during quiescent phases of the evolution of intermediate-mass stars (e.g. Wheeler et al. 1989), they should be detected only in those stars which were born after such intermediate-mass stars have had time to complete their evolution. The detection of such elements as barium in the atmospheres of the most extreme metal-poor stars thus led several investigators, following Truran (1981), to remark that, although the dominant isotopes of these elements in solar-system material are s-process products, most of them also have r-process isotopes. They then argued that it is just these r-process isotopes that we detect in the atmospheres of the most extreme metal-poor stars. This suggestion was supported by several recent determinations of heavy elements abundances in the atmospheres of metal-poor giants (Sneden & Parthasarathy 1983; Sneden & Pilachowski 1985; Gilroy et al. 1988).

However, the quasi-exclusive consideration of giant stars in these investigations introduces several uncertainties. First, one cannot definitely exclude that the chemical composition of the atmosphere of such stars has been perturbed as a result of some mixing of the surface gas with material already processed in the stellar interior (Wheeler et al. 1989). Their surface chemical composition would no longer be identical to that of the gas out of which they formed. Moreover, most of these giant stars are situated rather far away from us. Their light might thus have suffered some reddening by interstellar dust. As a consequence, their effective temperatures cannot be obtained with the same accuracy as for nearby dwarfs. The deduced abundance ratios are thus affected by larger uncertainties.

These considerations, reinforced by the hope that the increased precision of our data might reveal entirely new effects, prompted us to undertake a systematic analysis of the heavy elements abundances in metal-poor dwarfs. In this paper, we

present the results for two of the lightest among the neutron-capture elements, namely yttrium and zirconium.

The first systematic analysis of the Y abundance in very metal-poor stars was due to Spite & Spite (1978) who gathered data for 10 stars, mostly giants. They found yttrium to be overdeficient with respect to iron at metallicities [Fe/H] < -1.5 (we use the standard notation $[M1/M2] \equiv \log(M1/M2)_{star} - \log(M1/M2)_{sun}$). More recently, Gilroy et al. (1988) found a similar result for 19 stars, out of which 17 are giants. However, the star-to-star scatter is rather large (~ 0.2 dex). On the other hand, from an analysis of 17 metal-poor dwarfs, Magain (1989) obtained a solar Y/Fe ratio down to [Fe/H] ~ -2.5 followed by a decrease at lower metallicities. The scatter is here significantly smaller. The reason for the discrepancy between dwarfs and giants could not be identified with certainty.

The zirconium abundance was only considered in a few investigations. Magain (1989) reported a very significant over-abundance in metal-poor dwarfs: $[Zr/Fe] = +0.49 \pm 0.12$. From the data of Gilroy et al. (1988), we obtain $[Zr/Fe] = +0.24 \pm 0.21$. Both analyses thus indicate a higher than solar Zr/Y ratio in metal-poor stars. Such a behaviour does not easily fit into the current models, as both elements are thought to be synthesized by the same processes.

2. Observations and reductions

The analysis is based on spectra obtained with the Coudé Echelle Spectrometer (CES) fed by the 1.4 m Coudé Auxiliary Telescope (CAT) at the European Southern Observatory, La Silla, Chile. The short camera was used with a CCD detector (RCA SID 503, 1024×640 pixels of 15×15 μm each). The slit width was set to 2″, corresponding to a resolving power of the order of 60 000. The exposure times were chosen in order to reach a signal-to-noise ratio above 200 in all spectral regions. A total of 20 stars were observed. They were selected in order to obtain a good metallicity coverage below [Fe/H] ~ -0.8. The spectra were collected during four observing runs, from Aug. 1987 to Dec. 1989. They cover a range of 30 to 40 Å around the following central wavelengths: 4210, 4900, 5200 and 5250 Å. Additional spectra were also available for some of the stars.

The data reduction was carried out with the help of the IHAP facility running on a HP 1000 computer at ESO, Garching. It consisted in:

(1) background subtraction, on the basis of the mean level measured on the parts of the CCD not illuminated by the stellar light, thus including electronic bias and dark current as well as any source of diffuse light;

(2) flat-fielding, using the spectrum of an internal lamp;

(3) wavelength calibration, using the stellar lines themselves to define the calibration curve, thus automatically correcting for the radial velocity;

(4) definition of the continuum, in the form of a low order Spline fitted through a number (~ 20) of pre-defined continuum windows;

(5) equivalent width measurement, by Gaussian fitting and by direct integration, the first method being preferred for the weak lines and the second in the case of the stronger ones (for which the non-Gaussian damping wings contribute significantly to the equivalent width).

The measured equivalent widths (EWs) are listed in Table 1. At a S/N of 200, we expect the EW uncertainties due to the photon noise to amount to 0.5 mÅ. The actual uncertainties should, of course, be somewhat larger as other sources of error may play a significant role (in particular, the position of the continuum at the shortest wavelengths).

3. Method of analysis

We adopt a classical method of analysis, the abundance being deduced from each line by forcing the computed EW to agree with the observed one. The theoretical EW is computed by integration of the line profile, the latter being determined by solving the transfer equation in a model atmosphere, under the assumption of local thermodynamic equilibrium (LTE). The model atmosphere is interpolated in the grid of Magain (1983), which was computed with a version of the Gustafsson et al. (1975) programme.

The Y and Zr abundances are deduced from three lines of Y II and one line of Zr II. The 4209 Å Zr II line is the only one which is suitable for the determination of the Zr abundance in very metal-poor dwarfs: all the other lines are either too weak or blended. The Y II and Zr II oscillator strengths are well known thanks to the works of Biémont et al. (1981) and Hannaford et al. (1982). The damping constants γ_6 (unimportant for such weak lines) are computed according to the Unsöld formula (Gray 1976), multiplied by an enhancement factor $f_6 = 1.5$. The solar abundances of Y and Zr are taken from Anders & Grevesse (1989).

The iron abundance [Fe/H] is determined on the basis of weak Fe I lines. Following the results of Magain & Zhao (1990), who detected departures from LTE in low excitation Fe I lines, we use only lines with an excitation potential above 4 eV. The oscillator strengths are deduced from the solar lines, measured on the Liège atlas (Delbouille et al. 1973). The Holweger-Müller (1974) model is used in the solar analysis. The solar iron abundance, as determined with our line analysis programme using the data of Simmons & Blackwell (1982) amounts to 7.66 in the usual logarithmic scale with $\log A_H = 12.00$. This value is slightly different from the one used by Magain & Zhao (1990) due to the use of new partition functions for iron (Halenka & Grabowski 1982). The oscillator strengths of the high excitation lines are then obtained by forcing these lines to indicate the same abundance as the Simmons & Blackwell (1982) lines. A damping enhancement factor $f_6 = 1.4$, as determined by Magain & Zhao (1990), is used for the high excitation Fe I lines.

If the absolute iron abundance has to be deduced from Fe I lines, the abundances of Y and Zr relative to iron should be obtained by comparing the Y II and Zr II lines to Fe II lines. The Fe II oscillator strengths are also deduced from the solar spectrum, using the same technique as for the Fe I lines, but with a damping enhancement factor $f_6 = 1.2$. The latter was determined, as in Magain & Zhao (1990), by forcing lines of different strengths to indicate the same abundance in metal-poor stars relative to the Sun.

One Ti II and one Cr II line are also present on our spectra. For the purpose of comparing the heavy elements abundances to these elements too, their oscillator strengths were also determined from the solar spectrum. The unknown damping enhancement factor was set to $f_6 = 1.5$ in this case.

The atomic data for the lines used in the present analysis are summarized in Table 2.

Table 1. Equivalent widths

λ	HD 3567	12042	22879	25704	33256	59984	61902	63077	76932	78747	84937	97320	122196	140283	160617	166913	194598	203608	211998	218502
Fe I																				
4885.43	18.2	51.3	36.4	32.0	50.0	38.4	34.5	37.8	30.9	44.0	1.5	16.2	4.5	4.0	5.4	6.7	—	35.8	23.7	4.3
4886.34	18.5	54.7	36.7	30.1	51.5	41.1	37.2	40.2	33.7	47.0	—	18.7	6.5	2.0	4.5	9.4	—	39.2	25.7	5.5
4892.87	6.3	28.6	16.1	15.4	25.3	20.3	17.4	18.4	18.4	24.2	—	7.4	3.7	—	2.5	2.2	—	16.7	9.8	—
5196.07	16.4	50.5	33.2	27.9	48.0	36.3	33.0	36.0	30.2	46.4	—	15.5	5.6	1.0	4.9	7.4	17.4	34.3	22.8	4.3
5243.78	9.1	35.3	22.0	20.4	36.0	26.5	22.3	24.7	20.3	30.3	—	8.6	2.1	1.0	3.5	4.5	12.4	24.1	13.8	2.2
5852.22	—	18.2	8.6	8.7	—	—	—	—	—	—	—	—	—	—	—	—	5.9	9.3	4.6	—
5856.09	—	15.8	7.5	6.5	—	—	—	—	—	—	—	—	—	—	—	—	—	8.0	2.6	—
5859.59	12.8	55.0	30.0	25.5	—	—	—	—	—	—	—	—	4.9	—	—	6.3	—	33.5	17.4	—
5862.36	18.4	62.5	41.6	37.8	—	—	—	—	—	—	—	—	6.4	—	—	—	26.5	46.0	27.0	6.5
Fe II																				
5197.58	47.7	85.5	56.5	57.0	100.5	70.7	73.2	57.0	54.3	63.0	13.6	47.3	28.8	11.4	29.5	32.4	41.4	65.8	45.8	21.1
5234.63	55.5	86.7	60.8	58.5	107.5	74.0	76.0	61.8	61.6	62.0	14.5	51.7	31.2	—	31.0	38.4	—	69.0	51.5	26.5
5264.81	17.2	45.0	21.8	21.5	52.0	34.7	33.9	26.2	22.8	26.4	2.7	14.0	7.7	2.0	5.8	8.4	15.6	28.9	14.0	5.3
Ti II																				
5185.91	38.6	67.5	55.0	52.2	77.8	60.5	59.5	61.7	57.5	67.0	6.9	36.8	16.9	5.5	21.2	26.4	33.4	52.0	51.6	18.4
Cr II																				
5237.33	17.2	50.1	26.0	24.6	63.0	36.5	38.6	28.0	28.5	29.5	2.7	18.4	8.3	—	5.5	9.2	—	33.6	15.9	5.4
Y II																				
4883.69	21.5	59.8	39.7	31.6	65.4	42.3	39.5	40.6	40.4	40.6	3.2	21.7	8.5	1.0	10.8	17.5	—	34.8	38.5	6.5
4900.12	25.0	58.0	38.0	32.5	—	42.0	37.8	42.0	42.0	43.0	3.2	23.0	9.0	0.7	12.0	15.7	—	31.5	36.8	5.5
5200.41	8.4	34.3	19.7	12.1	41.0	19.0	20.4	15.8	20.7	23.7	—	7.0	2.0	0.6	3.0	4.6	4.5	14.4	17.8	3.0
Zr II																				
4208.99	—	39.0	33.8	26.2	49.0	32.5	28.5	33.6	35.9	32.5	3.3	—	9.0	1.3	10.5	14.8	18.5	24.0	39.0	7.7

Table 2. Line data

Elem.	λ	χ_{exc}	log (gf)	f_6	$W_\lambda(\odot)$
Fe I	4885.43	3.88	−1.11	1.4	79.9
Fe I	4886.34	4.15	−0.79	1.4	87.0
Fe I	4892.87	4.22	−1.31	1.4	53.4
Fe I	5196.07	4.26	−0.84	1.4	79.8
Fe I	5243.78	4.26	−1.11	1.4	63.8
Fe I	5852.22	4.55	−1.28	1.4	42.4
Fe I	5856.09	4.29	−1.67	1.4	34.3
Fe I	5859.59	4.55	−0.66	1.4	79.2
Fe I	5862.36	4.55	−0.45	1.4	94.5
Fe II	5197.58	3.23	−2.33	1.2	87.3
Fe II	5234.63	3.22	−2.33	1.2	87.7
Fe II	5264.81	3.33	−3.17	1.2	47.3
Fe II	6143.25	3.89	−2.86	1.2	40.0
Ti II	5185.91	1.89	−1.52	1.5	63.6
Cr II	5237.33	4.07	−1.13	1.5	53.0
Y II	4124.92	0.41	−1.50	1.5	20.1
Y II	4883.69	1.08	+0.07	1.5	58.9
Y II	4900.12	1.03	−0.09	1.5	55.3
Y II	5200.41	0.99	−0.57	1.5	37.6
Zr II	4208.99	0.71	−0.46	1.5	43.0

Table 3. Model parameters

HD	T_{eff}(K)	log g	[Fe/H]	v_t(km s^{-1})
3567	5990	3.60	−1.35	1.25
12042	6110	3.95	−0.50	1.50
22879	5810	4.10	−1.00	1.15
25704	5710	3.90	−1.15	1.35
33256	6300	3.60	−0.45	1.40
59984	5870	3.60	−0.90	*
61902	6040	3.50	−0.85	*
63077	5710	4.00	−0.90	*
76932	5810	4.10	−1.10	*
78747	5620	4.10	−0.90	*
84937	6190	3.80	−2.40	*
97320	6030	3.90	−1.35	*
122196	5860	3.40	−2.00	1.65
140283	5640	3.20	−2.70	1.55
160617	5920	3.60	−1.90	1.25
166913	6030	3.80	−1.70	1.65
194598	5930	4.10	−1.30	1.00
203608	6110	4.20	−0.80	1.50
211998	5230	3.20	−1.60	1.25
218502	6110	3.70	−1.90	1.40

*: 1.25 km s^{-1} adopted.

4. Determination of the atmospheric parameters

4.1. *Effective temperature*

The stellar effective temperatures T_{eff} are deduced from the Strömgren $b-y$ and Johnson $V-K$ colour indices, using the calibrations of Magain (1987). The $b-y$ measurements are from Carney (1983), Lindgren (private communication) and Schuster & Nissen (1988). The $V-K$ colours are taken from Carney (1983) or have been obtained by us with the ESO 1 m telescope on La Silla. The adopted effective temperatures are means of the two determinations and are listed in Table 3, together with the other atmospheric parameters.

4.2. *Surface gravity*

The surface gravities log g are determined by forcing the Fe II lines to indicate the same abundance as the high excitation Fe I lines. As, on one hand, [Fe/H] is given by the Fe I lines which are, to first order, insensitive to the choice of the surface gravity and as, on the other hand, all ionic lines have roughly the same sensitivity to log g (thus making [Y/Fe] and [Zr/Fe] independent of log g), the surface gravity is not a very critical parameter. Its determination should nevertheless not be neglected as it can have indirect effects on the abundances, e.g. through the microturbulence velocity.

4.3. *Microturbulence velocity*

The microturbulence velocities v_t are obtained by forcing a set of lines of the same element and same ionization stage but with different EWs to indicate the same abundance. If available, our preferred choice is a set of Ca I lines of 2.52 eV excitation potential with accurate oscillator strengths from Smith & Raggett (1981). See Magain & Zhao (1990) for details. When these lines are not available (the spectral regions containing them were not observed for all stars), the microturbulence velocity is determined from the high excitation Fe I lines if some of them are strong enough to present some sensitivity to v_t. In the other cases, a value of 1.25 km s^{-1} is adopted.

5. Results

The deduced abundances for the 20 programme stars are summarized in Table 4, while Figs. 1 and 2 show the variation of [Y/Fe] and [Zr/Fe] with [Fe/H]. It is immediately apparent that, although Y behaves like iron through most of the metallicity range considered, Zr is clearly underdeficient in stars with $-2.5 < [Fe/H] < -1.0$. The mean value and scatter for the two abundance ratios in that metallicity range amount to:

$[Y/Fe] = -0.06 \pm 0.11$ (10 stars)

and

$[Zr/Fe] = +0.21 \pm 0.12$ (9 stars).

Note that the mentioned scatter is not the standard deviation of the mean but the star-to-star scatter.

The drop of [Y/Fe] and [Zr/Fe] at very low metallicities, although indicated by the HD 140283 data only, is highly significant. Indeed, that star is quite bright and the S/N of our spectra is very high (~250). Moreover, we have a spectrum of another spectral region, containing a stronger Y II line (λ 4374.94,

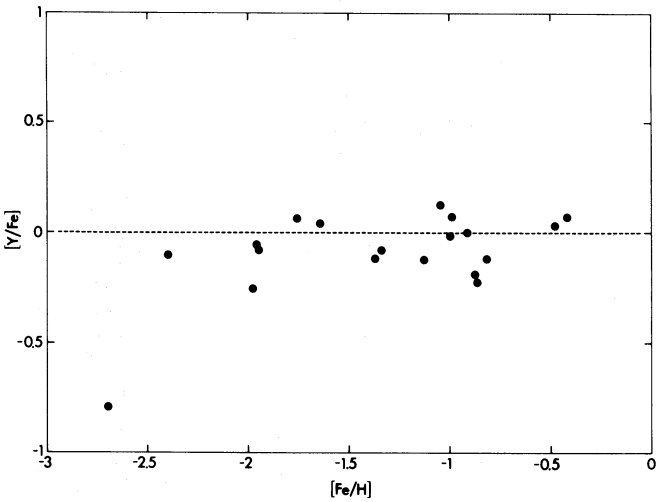

Fig. 1. Plot of [Y/Fe] versus [Fe/H]

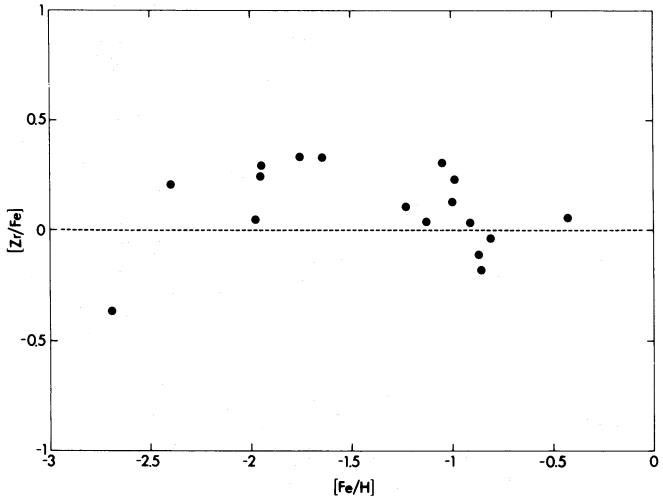

Fig. 2. Plot of [Zr/Fe] versus [Fe/H]

EW = 7.4 mÅ), so that the Y abundance is based on four lines giving consistent results. On the other hand, two measurements of the Zr II line on independent spectra agree within 0.2 mÅ.

While the Y II and Zr II oscillator strengths are laboratory measurements, the *gf* values for Fe I and Fe II are deduced from the solar spectrum. Moreover, the Holweger-Müller (1974) model is adopted for the Sun, while theoretical models are used for our programme stars. This is justified by our decision to carry out absolute analyses of the stars and not differential analyses with respect to the Sun (see Magain 1984, 1985, 1989 for discussions of the reasons for preferring absolute analyses). The Sun is thus used as a laboratory source and it is well known in that case that the Holweger-Müller model gives the best results (e.g. Sauval et al. 1984). However, for the purpose of comparing our results with the ones which would be found in a differential analysis, we computed the solar abundances from the same lines and atomic data, using the solar model from the same grid as the stellar models. The differences between these results and those obtained with the

Table 4. Element abundances

HD	[Fe/H]	[Ti/Fe]	[Cr/Fe]	[Y/Fe]	[Zr/Fe]
3567	−1.37	+0.21	—	−0.12	—
12042	−0.48	+0.08	−0.04	+0.03	—
22879	−0.99	+0.35	−0.01	+0.07	+0.24
25704	−1.13	+0.29	+0.04	−0.12	+0.04
33256	−0.43	+0.22	+0.07	+0.07	+0.06
59984	−0.87	+0.16	−0.08	−0.19	−0.11
61902	−0.86	+0.13	−0.08	−0.22	−0.18
63077	−1.00	+0.41	+0.02	−0.01	+0.13
76932	−1.05	+0.41	+0.10	+0.13	+0.30
78747	−0.91	+0.47	+0.02	+0.00	+0.04
84937	−2.31	+0.19	−0.06	−0.10	+0.20
97320	−1.34	+0.24	+0.02	−0.08	—
122196	−1.98	+0.12	+0.05	−0.25	+0.05
140283	−2.63	+0.06	—	−0.67	−0.36
160617	−1.96	+0.29	−0.13	−0.06	+0.24
166913	−1.76	+0.32	−0.01	+0.06	+0.33
194598	−1.23	+0.20	—	—	+0.11
203608	−0.81	+0.18	+0.03	−0.12	−0.04
211998	−1.65	+0.38	+0.04	+0.04	+0.33
218502	−1.95	+0.38	−0.03	−0.08	+0.29

Holweger-Müller model then correspond to the differences between a fully differential analysis and our present analysis. While the mean iron abundance (deduced from the Fe I lines) is lower by 0.09 dex (thus meaning higher [Fe/H] for our programme stars), the changes in the abundances given by the Fe II, Y II and Zr II lines are essentially the same (0.07 dex), thus leaving the relative abundances unchanged within 0.01 dex.

The uncertainties in our abundance estimates due to EW errors can be estimated by comparing the results from different lines. The typical scatter in the yttrium abundances as given by the three Y II lines amounts to 0.12 dex. This would correspond to a mean uncertainty of $0.12/\sqrt{3} = 0.07$ dex on [Y/H]. However, closer inspection reveals systematic differences between the abundances indicated by the three lines, the 4900 Å result being on the average 0.1 dex higher than the others. This might be due to errors in the laboratory oscillator strengths, although this value is somewhat larger than the published uncertainties (~0.03 dex, Hannaford et al. 1982). Correcting for these systematic differences, the line-to-line scatter is reduced to 0.04 dex, corresponding to a mean uncertainty of 0.02 dex on [Y/H]. A similar comparison of the three Fe II lines gives comparable results. Finally, assuming the same uncertainty on the EW of the single Zr II line as on the Y II EWs leads to a standard error of 0.04 dex on [Zr/H].

Errors on the adopted atmospheric parameters constitute another important source of uncertainty. The variation of the abundance ratios due to changes in effective temperature, surface gravity, model metallicity and microturbulence velocity are summarized in Table 5 for two typical cases. As expected, the main contribution to the total uncertainty comes from effective temperature errors, but it should never exceed some 10%.

The expected scatter in [Y/Fe] or [Zr/Fe] due to analysis uncertainties is thus of the order of 0.05 dex, which is two times less than observed. There is thus an additional source of scatter in

Table 5. Effect of the uncertainties in the atmospheric parameters on the deduced abundances

	HD 22879			HD 160617		
	[Fe/H]	[Y/Fe]	[Zr/Fe]	[Fe/H]	[Y/Fe]	[Zr/Fe]
$\delta T_{\rm eff} = -50$ K	−0.03	−0.02	−0.03	−0.03	−0.02	−0.02
$\delta \log g = +0.3$	+0.00	+0.00	+0.01	+0.01	−0.01	+0.00
δ[Fe/H] = +0.2	+0.00	+0.01	+0.00	+0.00	+0.00	+0.01
$\delta v_t = +0.25$	−0.02	+0.02	+0.02	−0.00	+0.01	+0.01
Rms sum	0.04	0.03	0.04	0.03	0.02	0.02

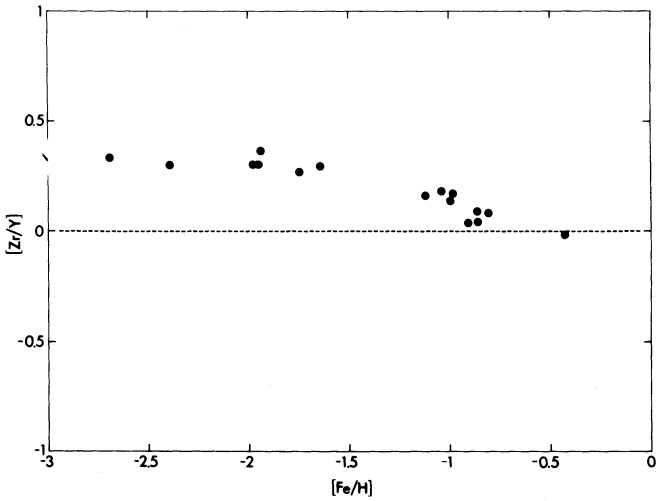

Fig. 3. Plot of [Zr/Y] versus [Fe/H]

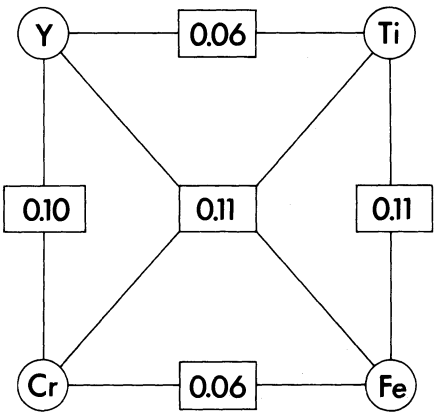

Fig. 4. The scatters in the various abundance ratios are shown along the lines connecting the different elements considered

these abundance ratios. This is confirmed by Fig. 3, which shows [Zr/Y] plotted as a function of [Fe/H]. Apart from a confirmation of the differences in the behaviour of these two elements, the most striking feature of Fig. 3 is the very small scatter in [Zr/Y], of the order of 0.03 dex only. This value is even smaller than what is expected from analysis uncertainties alone, probably indicating that our error estimates were somewhat too conservative.

There is thus a contribution to the scatter in [Y/Fe] and [Zr/Fe] which cannot be explained by obvious analysis uncertainties. We are thus left with two possibilities: either that scatter is cosmic and there are genuine differences in relative abundances from star to star at the same overall metallicity or that scatter is due to other effects, not taken into account in our work. Among these possible sources of scatter, one may mention departures from LTE or from plane parallel geometry – e.g. in the form of granulation – or even selective diffusion of the elements in the stellar atmospheres. In all these cases, one might expect some correlation between the abundance ratios and some atmospheric parameters. This is not confirmed by our results, which display no such correlation. More insight can be gained by comparing Y and Zr with Ti and Cr, two elements for which one ionic line is present in our spectra. The first ionization potentials of these two elements being more comparable to those of Y and Zr than is the case for Fe, one might expect a better cancelation of, e.g., granulation effects on these abundance ratios. The observed scatters are reported in Fig. 4 which shows that, if such a reduction of the scatter is indeed present in the comparison with Ti (see Figs. 5 and 6), this is not the case for Cr which correlates well with Fe, as expected on nucleosynthesis grounds. Note that the scatters in [Y/Ti], [Zr/Ti] and [Cr/Fe], although somewhat larger than the scatter in [Zr/Y], are not inconsistent with our expectations from analysis errors.

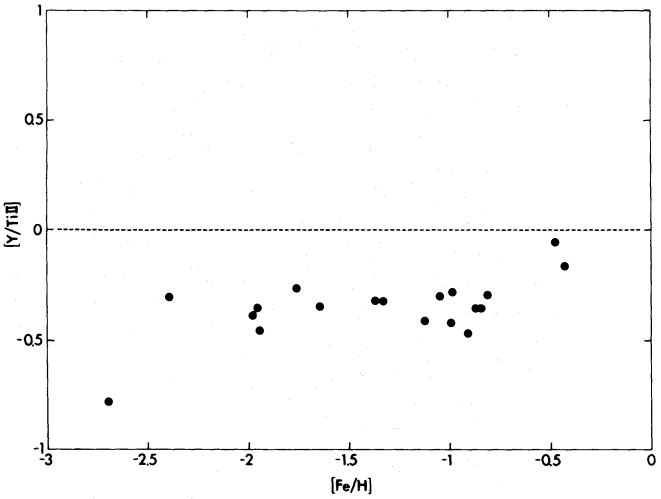

Fig. 5 Plot of [Y/Ti] versus [Fe/H]

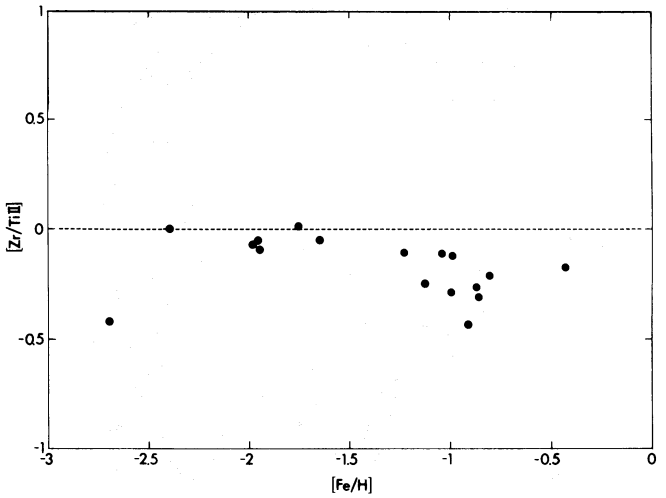

Fig. 6. Plot of [Zr/Ti] versus [Fe/H]

We can thus conclude that there is most probably a genuine cosmic scatter in [Y/Fe] and [Zr/Fe] (and in [Ti/Fe] as well). This scatter amounts to some 0.1 dex or a little less, in the metallicity range $-2<[Fe/H]<-1$.

6. Comparison with previous investigations

Before discussing the implications of our findings for the nucleosynthesis and galactic evolution models, it may be useful to compare them with the results of previous investigations. Table 6 gives the iron and yttrium abundances derived by several authors for the well studied subgiant HD 140283. It is immediately apparent that not only the [Y/Fe] but also the deduced [Fe/H] vary strongly from one investigation to the other.

The [Fe/H] values in the first two investigations were obtained by a differential analysis relative to the Sun, although Gilroy et al. (1988) themselves favour an absolute analysis, i.e. one using laboratory *gf* values, and adopt it for the neutron-capture elements. The possible systematic errors in such differential analyses have been commented on at length in previous papers (Magain 1984, 1985, 1989).

The slightly lower [Fe/H] obtained by Magain (1989) can probably be attributed to his use of mostly low excitation Fe I lines, probably affected by departures from LTE (Magain & Zhao 1990). The excellent agreement between the present determination and the recent one by Ryan et al. (1990) is partly fortuitous. Indeed, the latter authors use a higher effective temperature as well as many low excitation lines. These two factors probably lead to two compensating differences with respect to the present analysis.

Table 6. Comparison of the various analyses of HD 140283

Reference	[Fe/H]	[Y/Fe]
Spite & Spite (1978)	−2.40	−0.40
Gilroy et al. (1988)	−2.25	+0.08
Magain (1989)	−2.75	−0.58
Ryan et al. (1990)	−2.62	+0.48
This paper	−2.63	−0.67

Turning now to the Y abundance, the situation is even worse, differences over one order of magnitude being found between the various determinations. It should be noted that, apart from the present value of [Y/H] which is deduced from four lines, all the other results are based on one line only. Moreover, all past values of [Y/H], except the one from Magain (1989) are higher than our present determination. It is obvious that this results from systematic measurement errors: a weak line in a spectrum of insufficient S/N is considered only if it is reinforced by the noise and dropped in the other case. Although this is a well known source of systematic error, it is obviously not taken properly into account by many authors. We strongly caution against such kinds of systematic errors which are quite easy to avoid but generally not considered duly. Anyhow, this comparison suffices to show that previous results for Y should be considered with caution, at least for very metal-poor dwarfs in which the lines are so weak that only very high S/N spectra should be used.

Very few past investigations have addressed the problem of the Zr abundance in metal-poor stars. Gilroy et al. (1988) determined [Zr/H] from three lines of Zr II (two only being available in most stars). One of these lines is the same as considered here, while another one is very badly blended and the last one is quite weak. Their results show a very large scatter. As an example, their star-to-star scatter in [Zr/Y] amounts to 0.27 dex, which is one order of magnitude higher than our value. This alone suffices to cast some doubts on the quality of their results.

Magain (1989) used the single 4209 Å line. His results for [Zr/Y] show a slightly stronger increase with decreasing [Fe/H] than found here but the overall agreement is satisfactory and the scatter is also quite small (0.05 dex only). For two stars in common, namely HD 160617 and HD 166913, the Magain (1989) values are 0.25 dex higher than the present results. Differences in EWs account for roughly half of this discrepancy, while the remaining 0.1 dex may probably be attributed to the use of different oscillator strengths for the Fe II lines, which would also explain a similar discrepancy of 0.1 dex in [Y/Fe], as deduced from six stars in common.

Most of the discrepancies between the present results and those of past investigations can thus be explained either by the use of different methods of analysis or by the inaccuracies of the previous results for dwarf stars. The case of the giants is less clear. However, as far as the general trends are concerned, the results of Gilroy et al. (1988) are completely consistent with ours. The much larger scatter in their data could be due to the larger uncertainties in their analysis. These larger uncertainties can be explained both by the relatively lower quality of their data and by the fact that analyses of giant stars are affected by larger errors, e.g. in the determination of the effective temperature. However, it cannot be excluded that the increased scatter in the giant stars abundances is due to perturbations of their surface composition in the course of their evolution away from the main sequence. It should also be pointed out that, although the overlap is not negligible, the metallicity ranges sampled by these two investigations differ significantly. This is even more so if our results are to be compared with those of Ryan et al. (1990) which concern stars of much lower metallicities. The intercomparison of these different investigations might thus also indicate an increase of the scatter in

[Y/Fe] and [Zr/Fe] (but what about [Zr/Y]?) at the lowest metallicities.

7. Discussion and conclusions

One of the main results of our analysis is the difference in behaviour between the – supposedly similar in terms of nucleosynthesis – elements Y and Zr. Other important conclusions are the extremely low scatter in [Zr/Y] and the – relatively small but clearly measurable – cosmic scatter in [Y/Fe] and [Zr/Fe]. Also, the lower scatter in [Y/Ti] and [Zr/Ti] came as a completely unexpected result. We would like now to very briefly discuss these results and see if (and how) they can be understood in the framework of the current models of stellar nucleosynthesis and galactic evolution.

The most obvious way to interpret the variation of [Zr/Y] with [Fe/H] would be to assume a different contribution from the r and s-processes to these two elements, the fraction of Zr synthesized by the r-process being larger than for Y. This would explain the positive value of [Zr/Y] at the lowest metallicities, when the r-process is supposed to dominate, and the relatively faster increase of the Y abundance with [Fe/H], as the s-process contribution starts to become dominant. However, we feel that this relatively straightforward explanation cannot easily account for the extremely low – if any – scatter in [Zr/Y] at a given metallicity. Indeed, if two completely different processes played a significant role in the synthesis of these elements, it is a little hard to understand how they could do it in proportions which would be determined by the initial metallicity only and would depend on no other factor, such as the stellar mass.

Recent nucleosynthesis calculations (Prantzos et al. 1990) indicate that the lighter neutron capture elements, such as those considered here, can be produced in significant amounts by the s-process in massive stars, even at low metallicities. As, unlike Fe or Cr, Ti is generally considered to be synthesized by massive stars, the close correlation of Y and Zr with Ti (in terms of a low star-to-star scatter) could be interpreted as supporting these models. Massive stars could then be, via the s-process (but why not via the r-process too?), significant producers of the lighter neutron capture elements in the early stages of the galactic evolution. It would be very interesting to compare the present results with those for the heavier neutron capture elements, like Ba, which should not be – at least through the s-process – produced in significant amounts by such massive, short-lived stars. This will be one of the purposes of the next paper in this series.

References

Anders E., Grevesse N., 1989, Geochimica et Cosmochimica Acta 53, 197

Biémont E., Grevesse N., Hannaford P., Lowe R.M., 1981, ApJ 248, 867

Carney B.W., 1983, AJ 88, 623

Delbouille L., Neven L., Roland G., 1973, Photometric Atlas of the Solar Spectrum from 3000 Å to 10000 Å, Institut d'Astrophysique de l'Université de Liège, Belgium

Gilroy K.K., Sneden C., Pilachowski C.A., Cowan J.J., 1988, AJ 327, 298

Gray D.F., 1976, The Observation and Analysis of Stellar Photospheres, Wiley, New York

Gustaffson B., Bell R.A., Eriksson K., Nordlund Å., 1975, A&A 42, 407

Halenka J., Grabowski B., 1984, A&AS 57, 43

Hannaford P., Lowe R.M., Grevesse N., Biémont E., Whaling W., 1982, ApJ 261, 736

Holweger H., Müller E.A., 1974, Solar Phys. 39, 19

Magain P., 1983, A&A 122, 225

Magain P., 1984, A&A 134, 189

Magain P., 1985, A&A 146, 95

Magain P., 1987, A&A 181, 323

Magain P., 1989, A&A 209, 211

Prantzos N., Hashimoto M., Nomoto K., 1990, A&A 234, 211

Ryan S.G., Norris J.E., Bessell M.S., 1990, AJ (sumbitted)

Sauval A.J., Grevesse N., Brault J.W., Stokes G.M., Zander R., 1984, ApJ 282, 330

Schuster W.J., Nissen P.E., 1988, A&AS 73, 225

Simmons G.J., Blackwell D.E., 1982, A&A 112, 209

Smith G., Raggett D.St.J., 1981, J. Phys. B14, 4015

Sneden C., Parthasarathy M., 1983, ApJ 267, 757

Sneden C., Pilachowski C.A., 1985, ApJ 288, L55

Spite M., Spite F., 1978, A&A 67, 23

Wheeler J.C., Sneden C., Truran J.W., 1989, ARA&A 27, 279